Published OnlineFirst March 10, 2009; DOI: 10.1158/1541-7786.MCR-08-0056

p31^{comet} Induces Cellular Senescence through p21 Accumulation and Mad2 Disruption

Miyong Yun,[1,6] Young-Hoon Han,[1] Sun Hee Yoon,[1] Hee Young Kim,[1] Bu-Yeo Kim,[1] Yeun-Jin Ju,[1] Chang-Mo Kang,[2] Su Hwa Jang,[3] Hee-Yong Chung,[3] Su-Jae Lee,[4] Myung-Haing Cho,[5] Gyesoon Yoon,[8] Gil Hong Park,[6] Sang Hoon Kim,[7] and Kee-Ho Lee[1]

Laboratories of [1]Radiation Molecular Cancer and [2]Cytogenetics and Tissue Regeneration, Korea Institute of Radiological and Medical Sciences; Departments of [3]Microbiology and [4]Chemistry, Hanyang University College of Medicine; [5]Laboratory of Toxicology, College of Veterinary Medicine, Seoul National University; [6]Department of Biochemistry, College of Medicine, Korea University; [7]Department of Biology, Department of Life and Nanopharmaceutical Sciences, Kyung Hee University, Seoul, Korea and [8]Department of Biochemistry and Molecular Biology, Ajou University School of Medicine, Suwon, South Korea

Abstract

Functional suppression of spindle checkpoint protein activity results in apoptotic cell death arising from mitotic failure, including defective spindle formation, chromosome missegregation, and premature mitotic exit. The recently identified p31^{comet} protein acts as a spindle checkpoint silencer via communication with the transient Mad2 complex. In the present study, we found that p31^{comet} overexpression led to two distinct phenotypic changes, cellular apoptosis and senescence. Because of a paucity of direct molecular link of spindle checkpoint to cellular senescence, however, the present report focuses on the relationship between abnormal spindle checkpoint formation and p31^{comet}-induced senescence by using susceptible tumor cell lines. p31^{comet}-induced senescence was accompanied by mitotic catastrophe with massive nuclear and chromosomal abnormalities. The progression of the senescence was completely inhibited by the depletion of p21$^{Waf1/Cip1}$ and partly inhibited by the depletion of the tumor suppressor protein p53. Notably, p21$^{Waf1/Cip1}$ depletion caused a dramatic phenotypic conversion of p31^{comet}-induced senescence into cell death through mitotic catastrophe, indicating that p21$^{Waf1/Cip1}$ is a major mediator of p31^{comet}-induced cellular senescence. In contrast to wild-type p31^{comet}, overexpression of a p31 mutant lacking the Mad2 binding region did not cause senescence. Moreover, depletion of Mad2 by small interfering RNA induced senescence. Here, we show that p31^{comet} induces tumor cell senescence by mediating p21$^{Waf1/Cip1}$ accumulation and Mad2 disruption and that these effects are dependent on a direct interaction of p31^{comet} with Mad2. Our results could be used to control tumor growth. (Mol Cancer Res 2009;7(3):371–82)

Introduction

During cell division, sister chromatids are separated and distributed to each emerging daughter cell. Microtubules initially attach to generate accurate tension between the bio-oriented kinetochores (1, 2) and pull each chromatid to the respective daughter cell. This process requires reliable orchestration to ensure survival over generations. Consequently, cells are devised with mechanisms to fix and recover errors generated during division. One of these mechanisms is the spindle checkpoint, which is activated during mitosis to monitor attachment of sister chromatids to the spindle. When the spindle checkpoint is on, Mad2 is recruited to kinetochores and released in a modified form that interacts with Cdc20 (3) to form an inhibitory complex regulating APC/C-mediated ubiquitination of securin (4, 5). Following the completion of spindle attachment, Mad2 dissociates from the Cdc20-APC complex to silence the spindle checkpoint (6).

p31^{comet} was initially identified as a Mad2-interacting protein (7). It is proposed that p31^{comet} facilitates dissociation of Mad2 by transient interactions with the inhibitory Mad2-Cdc20-containing complexes to allow transition from the metaphase to anaphase during mitotic checkpoint inactivation. Other reports suggest that p31^{comet} enhances the activity of APC/C, which is otherwise inhibited by Mad2, without disrupting Mad2-Cdc20 binding in the transient Mad2-Cdc20-APC/C complex (8, 9). Both hypotheses concur that p31^{comet} counteracts Mad2 function and is required for silencing the spindle checkpoint.

Suppression of spindle checkpoint function is invariably lethal because of inadequate chromosomal segregation. For instance, functional inactivation of the BubR1 or Mad2 stimulates apoptotic cell death (10, 11). Mouse embryos deficient in BubR1 or Mad2 fail to survive because of extensive

Received 1/30/08; revised 11/7/08; accepted 11/17/08; published OnlineFirst 3/10/09.

Grant support: National Nuclear R&D Program and Human Genome Project grant FG-06-11-04 from Korean Ministry of Science and Technology; BAERI, Korea Ministry of Science and Technology (G.H. Park and S.H. Kim); and Korea Research Foundation from the Korean Government grant KRF-2006-311-E00507 (M-H. Cho).

The costs of publication of this article were defrayed in part by the payment of page charges. This article must therefore be hereby marked *advertisement* in accordance with 18 U.S.C. Section 1734 solely to indicate this fact.

Note: Supplementary data for this article are available at Molecular Cancer Research Online (http://mcr.aacrjournals.org/).

Current address for B-Y. Kim: Department of Medical Research, Korea Institute of Oriental Medicine, 483 Exporo, Yuseong-gu, Daejeon 305-811, Korea.

Requests for reprints: Kee-Ho Lee, Laboratory of Radiation Molecular Cancer, Korea Institute of Radiological and Medical Sciences, 215-4 Gongneung-dong, Nowon-Ku, Seoul 139-706, Korea. Phone: 82-2-970-1312/1314; Fax: 82-2-970-2402. E-mail: khlee@kcch.re.kr

doi:10.1158/1541-7786.MCR-08-0056

Published OnlineFirst March 10, 2009; DOI: 10.1158/1541-7786.MCR-08-0056

apoptosis (12, 13). Moreover, mutation of *Bub1* leads to chromosomal missegregation and failure to block apoptosis in *Drosophila* (14). These findings collectively illustrate that apoptosis derived from the loss of spindle checkpoint function contributes to protection against the emergence of an aberrant cell population.

Although cellular senescence, together with apoptosis, is a major additional safeguard mechanism, direct evidence that functional attenuation of spindle checkpoint proteins activates the senescence pathway has recently been found by using a mouse model system. The reduced amounts of the BubR1 protein result in the early onset of cellular senescence and accelerate the aging process of mice (15, 16). The combined alteration by Bub3 and Rae1 of the mitotic checkpoint also prominently affects the cellular and organismal processes of senescence and aging (17). Based on alterations in cellular physiology, it has been established that spindle checkpoint proteins are closely connected with cellular senescence. Several anticancer drugs targeting the microtubule, such as Taxol and vincristine, induce senescence-like phenotypes due to abnormal mitosis in a variety of tumor cells (18-20). Senescence of a fibrosarcoma cell line triggered by $p21^{Waf1/Cip1}$ is associated with depletion of the cellular pools of mitotic control proteins, such as Mad2, BubR1, cyclin B1, and Cdc2 (21). The induction of senescence-like phenotypes in cancer cells is accompanied by mitotic catastrophe (21). These various plausible interconnections between spindle checkpoint and cellular senescence request to identify their connecting molecules, the elucidation of which can enable to explain the physiologic details.

Based on the interactions between $p31^{comet}$ and Mad2, we propose that $p31^{comet}$ functions in inducing cellular senescence. Our data show that $p31^{comet}$ overexpression is associated with senescence-like morphologic changes and senescence-associated β-galactosidase (SA-β-gal) expression. Induction of senescence by $p31^{comet}$ is exclusively dependent on disruption of Mad2 and accumulation of $p21^{Waf1/Cip1}$. These findings contribute significantly toward establishing the molecular mechanism of senescence derived from abnormal mitosis, which may be exploited to eliminate tumor cells effectively.

Results

$p31^{comet}$ Overexpression Induces Senescence-Like Phenotype and Apoptosis

To analyze the possible functional effects of $p31^{comet}$, we introduced the full-length human gene (7) into a bicistronic retroviral expression system coexpressing enhanced green fluorescent protein (EGFP) or puromycin as a selectable marker (Supplementary Fig. S1A). The resulting constructs, termed $p31^{comet}$-IRES-EGFP and $p31^{comet}$-IRES-puro, were retrovirally transduced into A549. The infectivity of $p31^{comet}$-IRES-EGFP and corresponding control-IRES-EGFP retroviral constructs was >89% as determined by counting cells displaying green fluorescence (Supplementary Fig. S1B).

Overexpression of $p31^{comet}$ in A549 cells led to enlargement of cells with a flattened shape (Fig. 1A) and multinuclei formation in a cell (Fig. 1B), which are the general characteristics of cellular senescence. Accordingly, we determined whether the $p31^{comet}$-mediated morphologic changes are due to cellular senescence. SA-β-gal activity was measured as a biomarker for cellular senescence in cells transduced with $p31^{comet}$. As predicted, $p31^{comet}$ overexpression was associated with increased SA-β-gal activity (Fig. 1B). The $p31^{comet}$-mediated SA-β-gal activity was evident 4 to 6 days after transduction and reached a level of 78% after 9 days, whereas control vector transduction failed to induce SA-β-gal activity (Fig. 1C). Among the β-gal-positive cells, 92% contained multiple nuclei ($n \geq 2$), whereas only 8% had a single nucleus. The maximal percentage of SA-β-gal-positive cells with multiple nuclei was recorded at 6 days after $p31^{comet}$ transduction and remained constant thereafter. Live cell imaging showed that $p31^{comet}$ inhibited cytokinesis during telophase (Supplementary Fig. S2), further supporting the idea that $p31^{comet}$ activates a pathway that results in accumulation of multinucleate cells. An increase in granularity is generally caused by accumulation of lipofuscin and other lipoprotein granules in the cytoplasm, which is also the characteristic of senescent cells (22). Granularity, presented as a 90° light scatter in flow cytometry analysis, was dramatically increased following $p31^{comet}$ transduction (Fig. 1D). To exclude the possibility that only extremely high levels of $p31^{comet}$ can induce senescence, we gradually reduced the level of $p31^{comet}$ overexpression by adding $p31^{comet}$ small interfering RNA (siRNA) in a dose-dependent manner to cells receiving $p31^{comet}$. This experiment showed that $p31^{comet}$ could induce senescence even when the overexpression level of the protein was reduced up to 5-fold (Supplementary Fig. S3). Thus, our present results clearly indicate that $p31^{comet}$ induces senescence-like phenotypes in A549 cells along with multinucleation. Similar $p31^{comet}$-mediated acquisition of SA-β-gal activity, flattened shape and multinucleation were evident in human lung cancer cell line Calu-1 (Supplementary Fig. S4) and human osteosarcoma cell line U2OS (Fig. 2A; data not shown). However, large amounts of HeLa and Hep3B cells underwent cell death, including apoptosis and necrosis, on $p31^{comet}$ overexpression (Fig. 2B). In contrast to plenty of the molecular association between abnormal spindle checkpoints and apoptosis, there is a limited understanding of its molecular link directly to senescence, as it has recently been reported in the cases of BubR1 insufficiency (15, 16) and Bub3/Rae1 double haploinsufficiency (17). In the present study, therefore, we focused on $p31^{comet}$-induced senescence using a highly susceptible A549 cell line.

$p31^{comet}$ Overexpression Is Associated with Complete Regression of Clonal Cell Growth

Next, we examined whether $p31^{comet}$-mediated senescence influences cellular proliferation. Transduction of $p31^{comet}$ led to a significant reduction in cellular proliferation, whereas the control vector did not affect the growth rate (Fig. 3A). In a clonal cell growth assay, $p31^{comet}$ had a profound effect on colony formation. Cells transduced with the $p31^{comet}$-IRES-EGFP retroviral vector formed only 25 colonies, none of which were EGFP-positive, indicating that the cells transduced with $p31^{comet}$ did not form colony. In contrast, control-IRES-EGFP retroviral vector transduction produced 436 colonies, 401 of which were EGFP-positive (Fig. 3B). In view of this finding,

Published OnlineFirst March 10, 2009; DOI: 10.1158/1541-7786.MCR-08-0056

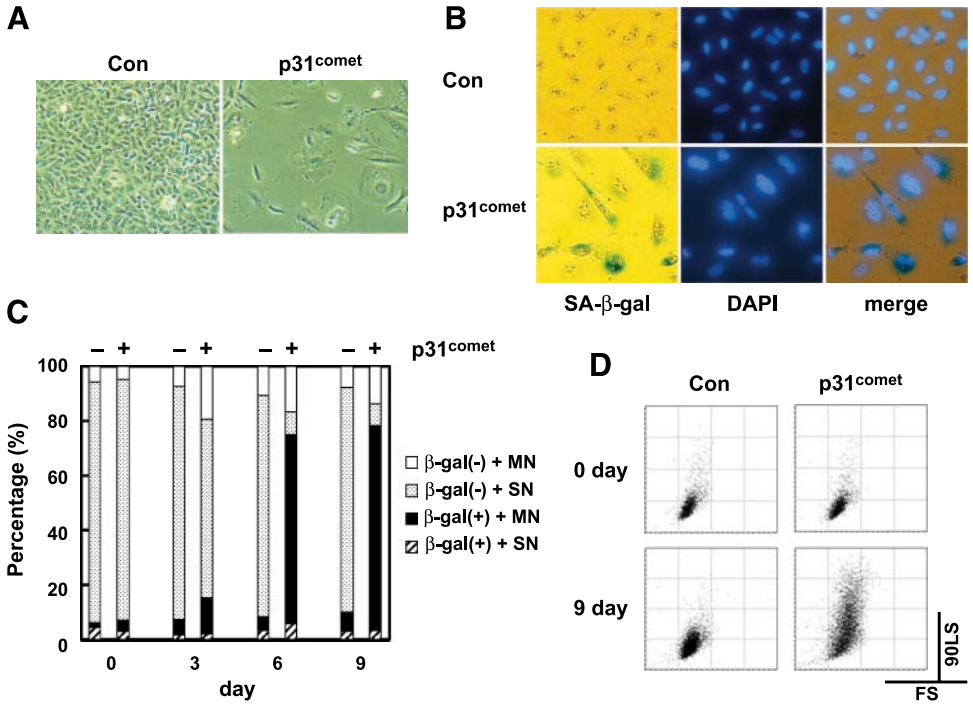

FIGURE 1. p31comet overexpression induces cellular senescence. **A.** Alteration of cell morphology by p31comet. A549 cells were infected with p31comet or control retrovirus at a multiplicity of infection of 8, and infected cells were photographed after 8 d. **B.** Microscopic analysis of SA-β-gal expression and multinucleation induced by p31comet. At 8 d after infection with p31comet or control retrovirus, SA-β-gal expression was assayed and cells were counterstained with 4′,6-diamidino-2-phenylindole solution. Bright-field images for SA-β-gal activity and fluorescent images for 4′,6-diamidino-2-phenylindole staining were acquired using an inverted fluorescence microscope from the same field. **C.** Time course for the accumulation of SA-β-gal-positive and multinucleated cells after p31comet transduction. At the indicated days after virus infection, cells were scored for SA-β-gal activity and nucleus number by counting 400 cells per dish. MN, multinucleated cells (including binucleated cells); SN, single nucleated cells. **D.** Flow cytometric analysis of p31comet-transduced cells. At 9 d after virus infection, cells were harvested and analyzed for forward light scatter (*FS*) and 90° light scatter (*90LS*).

we propose that p31comet elicits complete regression of colony formation. Flattened cells were subcultured for another 30 days to determine whether arrested cells ultimately undergo death. Interestingly, a large proportion of cells (80-90%) were metabolically active over the test period (data not shown). Evidently, p31comet overexpression hampers cell growth, eventually leading to permanent arrest.

p31comet-Mediated Senescence Is Accompanied by Stimulation of Cell Cycle Inhibitors and Senescence Marker Proteins

Senescence is generally accompanied by the induction of tumor suppressor and cell cycle inhibitor proteins, such as p53 (23, 24), $p16^{Ink4a}$ (25), $p21^{Waf1/Cip1}$ (26), and $p27^{Kip1}$ (27). Accordingly, we conducted Western blot analyses to determine whether p31comet-induced senescence involves the participation of tumor suppressors and cell cycle inhibitors. p31comet expression, which is very low at the basal level, was visible 24 h after transduction and sustained over the 8-day test period (Fig. 4A). Overexpression of p31comet led to elevation of the $p21^{Waf1/Cip1}$ protein level, which was evident 2 days after the transduction. The p53 tumor suppressor protein, a transcriptional regulator of $p21^{Waf1/Cip1}$ (28), was also significantly increased over a similar period. In contrast, we observed no changes in the expression pattern of $p27^{Kip1}$ protein, another known cell cycle inhibitor associated with senescence (29). Consistent with previous reports, we could not detect $p16^{Ink4a}$ protein that is defective in the A549 cell line (30). The present findings indicate that p31comet-mediated senescence is closely associated with p53 and $p21^{Waf1/Cip1}$ accumulation.

In addition to cell cycle inhibitors, cells undergoing senescence produce several common marker proteins, such as osteonectin, PAI-1, and SM22 (31, 32). To evaluate whether these marker proteins are stimulated in p31comet-mediated senescence, we examined their mRNA levels by reverse transcription-PCR after retroviral transduction. The mRNA levels of these markers were markedly elevated over the monitoring period in p31comet-transduced cells in contrast to little or no changes in control cells (Fig. 4B). We propose that p31comet overexpression triggers senescence with typical characteristics.

$p21^{Waf1/Cip1}$ Mediates the Phenotypic Conversion of p31comet-Induced Senescence to Death through Mitotic Catastrophe

As mentioned above, both p53 and $p21^{Waf1/Cip1}$ were up-regulated in p31comet-induced senescent A549 cells (Fig. 4A). Because $p21^{Waf1/Cip1}$ and p53 are cell cycle inhibitors, we predicted that the up-regulation of one or both of these proteins contributes to senescence. To confirm this theory, we examined whether down-regulation of either protein affects senescence induced by p31comet. Cells were transfected with $p21^{Waf1/Cip1}$ or

Published OnlineFirst March 10, 2009; DOI: 10.1158/1541-7786.MCR-08-0056

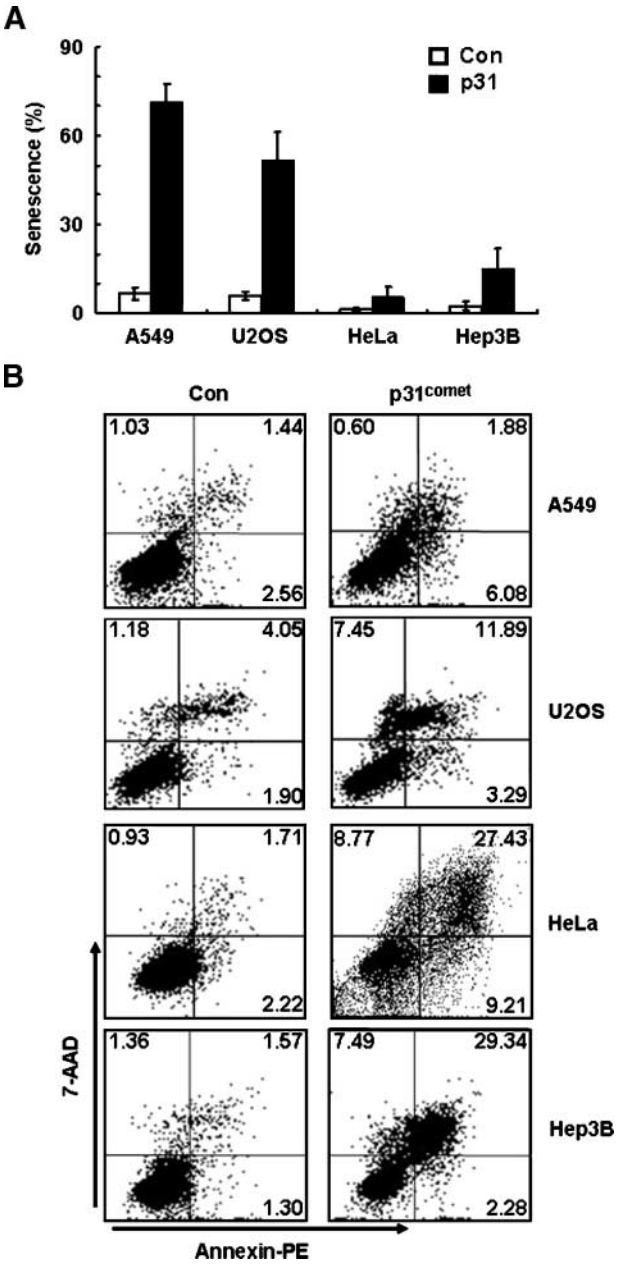

FIGURE 2. Senescence and death induced by p31^{comet}. **A.** Senescence profile determined by SA-β-gal staining. SA-β-gal-positive cells were scored from 400 cells 6 d after virus infection with p31^{comet}. The infectivity of A549, U2OS, HeLa, and Hep3B cells was 89.6%, 76.0%, 75.3%, and 76.2%, respectively. **B.** Cell death profile determined by 7-amino-actinomycin D and Annexin V-PE double staining. Death of A549, U2OS, HeLa, and Hep3B cells was determined by flow cytometry after Annexin V-PE and 7-amino-actinomycin D double staining 3 d after p31^{comet} infection.

p53 siRNA at 48 h after transduction with p31^{comet}. The resulting protein levels were successfully decreased (Fig. 5A). Depletion of p21$^{Waf1/Cip1}$ completely blocked p31^{comet}-induced senescence as revealed by dramatic reversion in the percentage of SA-β-gal-positive cells to the basal level (Fig. 5B). Evidently, induction of p21$^{Waf1/Cip1}$ is a critical step in p31^{comet}-mediated senescence. However, p53 depletion induced a smaller decrease in the percentage of SA-β-gal-positive cells, indicating a limited effect on p31^{comet}-induced senescence (Fig. 5B). Depletion of p53 additionally led to a decrease in the p21$^{Waf1/Cip1}$ protein level to some extent, consistent with the finding that p21$^{Waf1/Cip1}$ is a downstream target of p53. Thus, the observed effect of p53 depletion on p31^{comet}-induced senescence is possibly attributable to a concurrent reduction in levels of p21$^{Waf1/Cip1}$.

Next, we performed cell death experiments to determine if p31^{comet} expression might give rise to a cell population undergoing death. Cell death analysis using trypan blue staining (data not shown) and Annexin V/7-amino-actinomycin D staining analysis by fluorescence-activated cell sorting revealed that, whereas p31^{comet} induced mostly cellular senescence (Fig. 1C), p31^{comet} expression also resulted in the death of ~8% to 15% of cells during the interval of 5 days after transduction (Fig. 2B; data not shown). In the experiments involving p21$^{Waf1/Cip1}$ or p53 depletion described above, however, we found a marked phenotypic conversion of adherent senescent cells into floating dead cells. As anticipated from the clear reduction in the senescent population, both p21$^{Waf1/Cip1}$ and p53 depletion led to noticeable increases in cell death; in addition, p21$^{Waf1/Cip1}$ depletion resulted in more cell death than did p53 depletion (Fig. 5C and D). Specifically, dead cells after p21$^{Waf1/Cip1}$ depletion were composed of 21.5% necrotic and 34.5% apoptotic cells 6 days after p31^{comet} transduction. A malfunction of mitotic checkpoint regulators

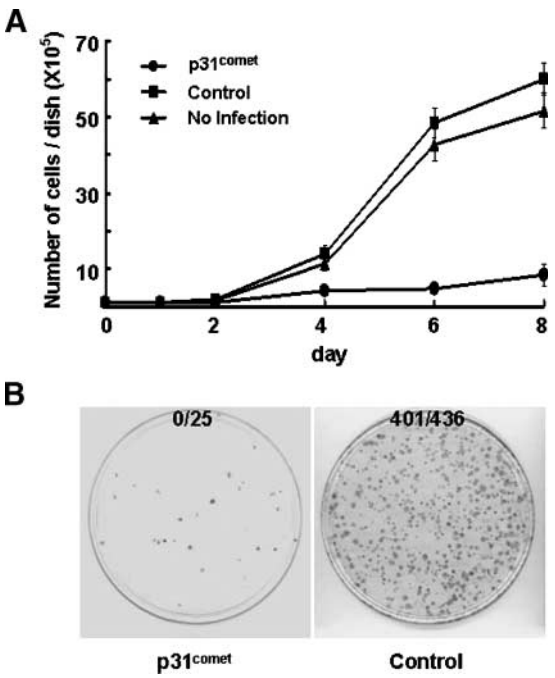

FIGURE 3. Irreversible growth inhibition by p31^{comet}. **A.** Inhibition of cell growth by p31^{comet}. A549 cells were infected with retroviruses containing p31^{comet} or control vector, and cell numbers were counted at the indicated days. **B.** Inhibition of colony-forming ability by p31^{comet}. A549 cells were infected with retroviruses containing p31^{comet}-IRES-EGFP or IRES-EGFP plasmid. Cells were plated at a density of 1×10^4 per 100 mm dish 2 d after virus infection. Colonies were stained with crystal violet.

Published OnlineFirst March 10, 2009; DOI: 10.1158/1541-7786.MCR-08-0056

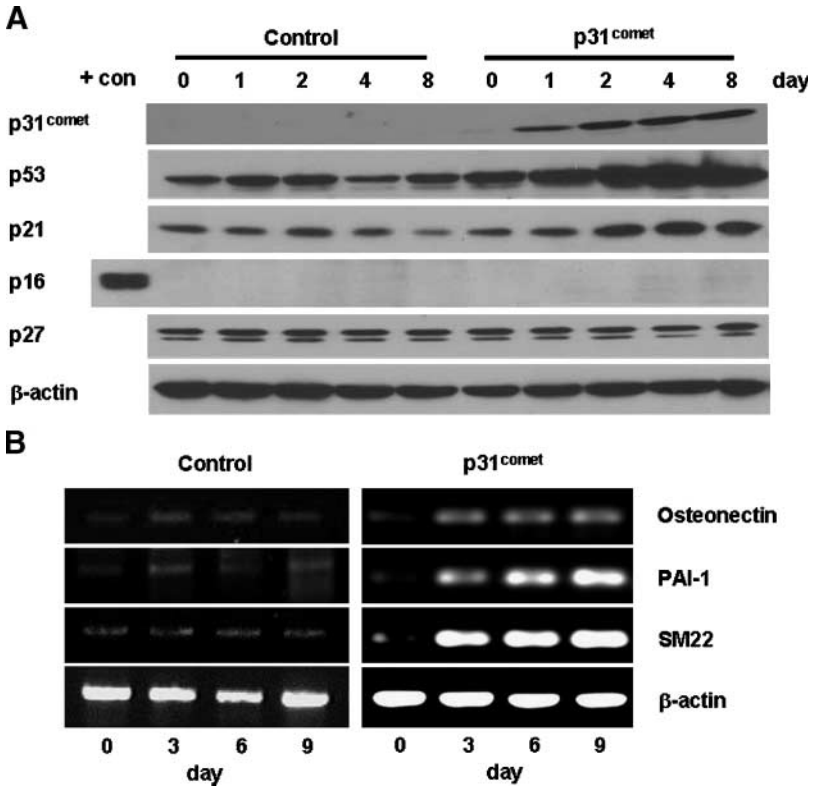

FIGURE 4. Expression of senescence-associated markers increases during p31^{comet}-induced senescence. **A.** Induction of p21$^{Waf1/Cip1}$ and p53 protein expression by p31^{comet}. A549 cells infected with retroviruses containing p31^{comet} or control vector were harvested at the indicated days and analyzed for expression of cell cycle inhibitor and tumor suppressor proteins by Western blot analysis. Cell lysates of p31^{comet}-transduced HeLa were included as a positive control for p16^{Ink4a} expression. **B.** Induction of mRNA associated with cellular senescence by p31^{comet}. Total RNA was prepared from A549 cells transduced with p31^{comet} or control vectors at the indicated days, and reverse transcription-PCR was done as described in Materials and Methods.

generates massive chromosomal and nuclear morphologic changes; this process is termed mitotic catastrophe (33, 34). As shown in Fig. 6A, together with multinuclei, micronuclei and anaphase bridges, which are the typical phenomenon of mitotic catastrophe, were seen in response to p31^{comet} overexpression. The frequency of anaphase bridge formation was ~8.3% after 1 day and 15.6% after 3 days following p31^{comet} transduction (Fig. 6B). Moreover, p31^{comet} caused a centrosome imbalance, in which cells receiving p31^{comet} had a higher number of centrosomes than cells with empty vectors (Supplementary Fig. S5). These findings indicate that p31^{comet}-induced senescence is accompanied by mitotic catastrophe with massive nuclear and chromosomal abnormality. The effect of p21$^{Waf1/Cip1}$ depletion was negligible on the formation of these nuclear and chromosomal aberrations. Thus, our present observation on the results of p21$^{Waf1/Cip1}$ or p53 depletion is that p21 is a major mediator in blocking phenotypic conversion of p31^{comet}-induced senescence to cell death through mitotic catastrophe. Thus, p21 functions as a negative regulator of cell death through mitotic catastrophe.

DNA Content Alterations and Decrease of Mad2 Expression by p31^{comet}

We conducted fluorescence-activated cell sorting analyses to monitor changes in the DNA content of cells infected with the p31^{comet} retrovirus. The proportion of cells (62%) in the G_0-G_1 phase decreased gradually to 58% and 33.5% at 4 and 9 days after p31^{comet} transduction, respectively (Fig. 7A and B). In contrast, a marked increase in the hyperploid cell population (>4N DNA) was evident (Fig. 7A and B). The nuclear and chromosomal aberration analysis showing the production of multinuclei (Figs. 1B and C and Fig. 6A), anaphase bridges (Fig. 6A), and centrosome imbalance (Supplementary Fig. S5), which are the evidences of ploidy changes, further supports the emergence of the hyperploid population caused by p31^{comet}. The increased hyperploidy was not observed in cells infected with control retrovirus. The data indicate that multinucleation due to p31^{comet} overexpression is part of the mechanistic basis for senescence induction. The majority of the hyperploid population underwent cellular senescence with the acquisition of SA-β-gal activity and maintained metabolic activity (data not shown). In addition to increase of hyperploid population, we found a small fraction of sub-G_0-G_1 peaks (Fig. 7A and B), further supporting that apoptotic cell death is also occurring as assessed in Figs. 2B and 5C.

Finally, to verify the endogenous expression of mitotic checkpoint regulators by p31^{comet}, we analyzed, over time, cells induced with p31^{comet}. We found that Mad2 and cyclin B1 expression gradually decreased, but there was no change in BubR1, p55Cdc, or Aurora B expression (Fig. 7C). When the expression of p21$^{Waf1/Cip1}$ and Mad2 (Figs. 4A and 7C) were compared, we noticed that p21$^{Waf1/Cip1}$ up-regulation preceded Mad2 down-regulation in p31^{comet}-induced senescence. Therefore, we examined whether p31^{comet}-induced Mad2 down-regulation might be dependent on p21$^{Waf1/Cip1}$. As shown in Fig. 7D, p21$^{Waf1/Cip1}$ depletion restored Mad2 expression that has been down-regulated by p31^{comet}, indicating that p21$^{Waf1/Cip1}$ is required for Mad2 down-regulation during p31^{comet}-induced senescence. Additionally, we show that Mad2

Published OnlineFirst March 10, 2009; DOI: 10.1158/1541-7786.MCR-08-0056

depletion itself also led to p21$^{Waf1/Cip1}$ up-regulation as caused by excess p31^{comet} (Supplementary Fig. S6), implying that the endogenous level of Mad2 successfully inhibits the induction of p21$^{Waf1/Cip1}$ expression. Thus, excess p31^{comet} appears to mimic Mad2 depletion via their interaction, thereby inactivating the ability of Mad2 to inhibit p21$^{Waf1/Cip1}$ induction. Accordingly, we conclude that p31^{comet} triggers senescence through p21$^{Waf1/Cip1}$ accumulation and downstream events that follow from Mad2 down-regulation.

Mad2 Disruption by p31^{comet} Is Responsible for Tumor Cell Senescence

At present, p31^{comet} is the recognized binding and regulatory partner of Mad2 that activates the mitotic checkpoint (7). Thus, we determined whether inactivation of Mad2 by complex formation with p31^{comet} is involved in senescence. Mad2 expression was initially depleted by siRNA transfection to analyze whether its down-regulation mimics conditions of p31^{comet} overexpression in inducing cellular senescence. To avoid the activation of the IFN system by siRNA (35), three different Mad2 siRNAs, which can deplete >80% of the basal level (Fig. 8A; data not shown), were applied and SA-β-gal activity was measured. As with p31^{comet} overexpression, the introduction of all three Mad2 siRNAs led to acquisition of SA-β-gal activity in A549 cells (Fig. 8B and D). In experiments using M2-2, a Mad2 siRNA, cell growth inhibition (Fig. 8E) and p21$^{Waf1/Cip1}$ accumulation (Supplementary Fig. S6) were clearly observed. The similar consequences of p31^{comet} overexpression and Mad2 down-regulation support our hypothesis that inhibition of Mad2 function is predominantly involved in the mechanism of p31^{comet}-induced senescence. To further verify these results, p31^{comet} mutants defective in interactions with Mad2 were employed. We designed a retroviral construct for a p31^{comet} mutant lacking 11 amino acids (residues 55-65) of the Mad2 binding site, denoted p31ΔM2, and confirmed expression at the appropriate level and size (Fig. 8C). In contrast to wild-type p31^{comet}, p31ΔM2 failed to induce senescence phenotypes, such as SA-β-gal activity (Fig. 8D), cell growth retardation (Fig. 8E), and flattened shape (data not shown). In addition, this mutant did not effectively down-regulate Mad2 expression compared with p31^{comet} wild-type (Fig. 8F), indicating that interaction between p31^{comet} and

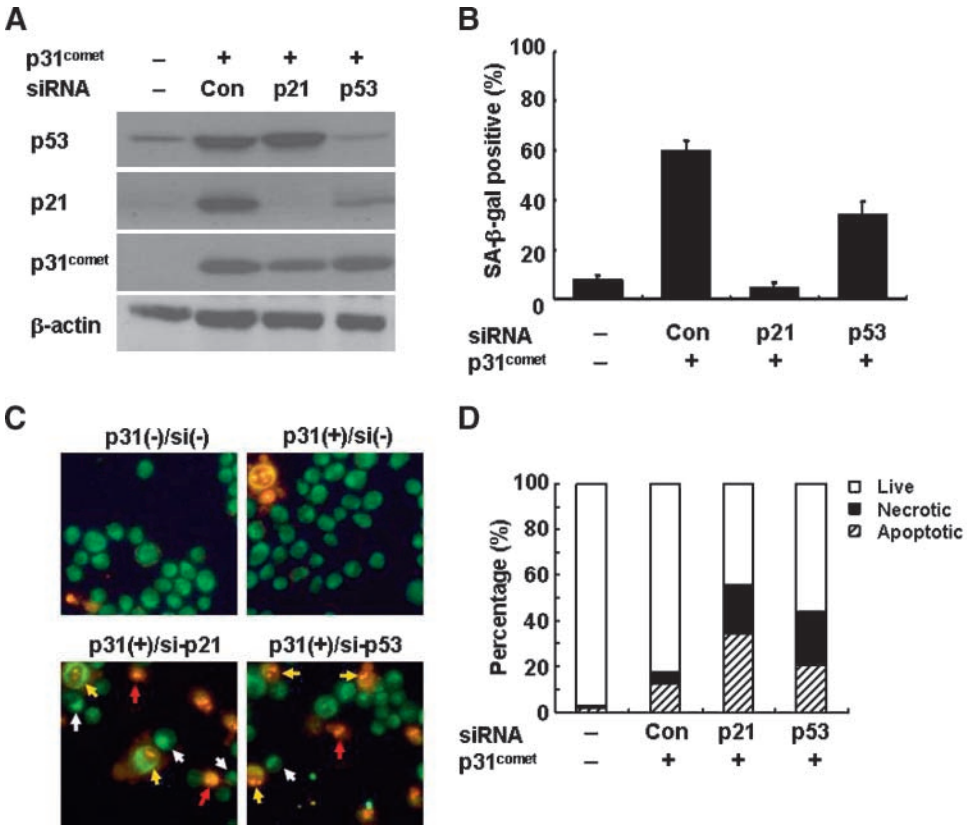

FIGURE 5. p21$^{Waf1/Cip1}$ expression is critical for p31^{comet}-mediated senescence. **A.** Suppression of p31^{comet}-mediated induction of p21$^{Waf1/Cip1}$ and p53 by siRNA transfection. siRNAs for p21$^{Waf1/Cip1}$ or p53 were transfected twice at 3-day intervals into p31^{comet}-transduced A549 cells. Total cell extracts were loaded and analyzed for the expression of p21$^{Waf1/Cip1}$ and p53 by Western blotting. β-Actin expression was used as a loading control. **B.** Complete inhibition of p31^{comet}-mediated senescence by suppression of p21$^{Waf1/Cip1}$ expression. siRNAs were transfected as described in **A**, and SA-β-gal-positive cells were scored as described in Fig. 2A after virus infection or siRNA transfection. **C.** Representative image of p31^{comet}-mediated cell death as shown by acridine orange-ethidium bromide double staining. siRNAs for control, p21$^{Waf1/Cip1}$, or p53 genes were transfected as described in **A**, and type of cell death was determined by differential nuclear staining using acridine orange and ethidium bromide. Different classes of nuclei were distinguished: live, uniformly green; showing early apoptosis, green with bright green dots (*yellow arrow*); showing late apoptosis, orange (*yellow arrowhead*); and showing necrosis, red (*red arrowhead*). **D.** Increase in p31^{comet}-mediated cell death by depletion of p21$^{Waf1/Cip1}$ or p53 expression. siRNAs for control, p21$^{Waf1/Cip1}$, or p53 were transfected as described in **A**, and live and apoptotic cell levels were calculated as in **C**.

Published OnlineFirst March 10, 2009; DOI: 10.1158/1541-7786.MCR-08-0056

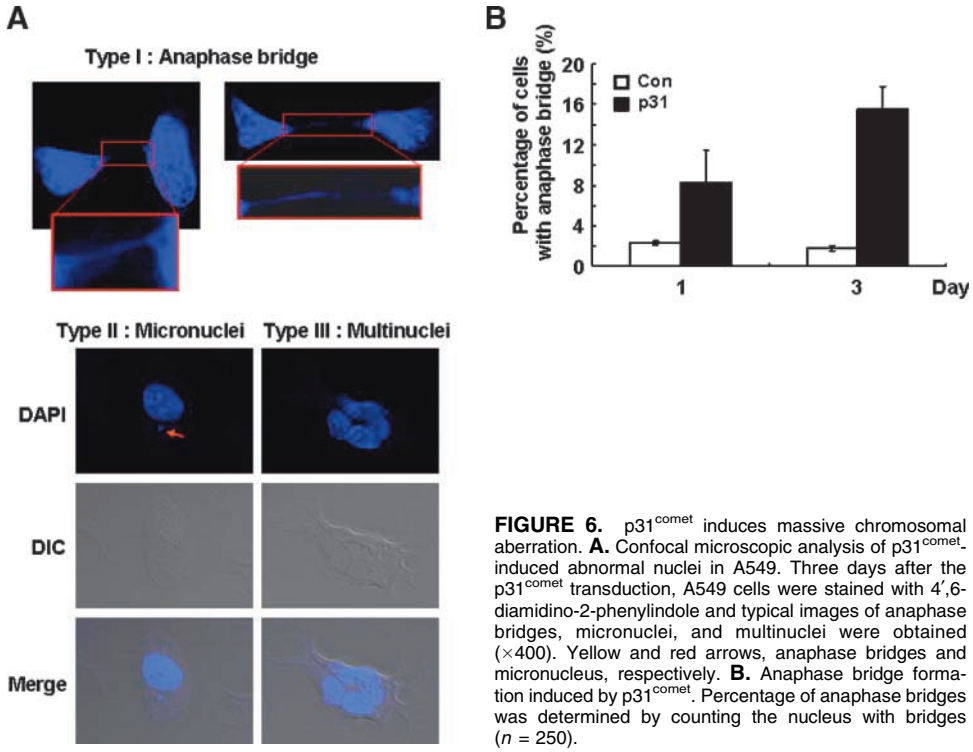

FIGURE 6. p31^{comet} induces massive chromosomal aberration. **A.** Confocal microscopic analysis of p31^{comet}-induced abnormal nuclei in A549. Three days after the p31^{comet} transduction, A549 cells were stained with 4′,6-diamidino-2-phenylindole and typical images of anaphase bridges, micronuclei, and multinuclei were obtained (×400). Yellow and red arrows, anaphase bridges and micronucleus, respectively. **B.** Anaphase bridge formation induced by p31^{comet}. Percentage of anaphase bridges was determined by counting the nucleus with bridges (n = 250).

Mad2 is required for Mad2 down-regulation. To further delineate whether the observed senescence might be derived from the fluctuation of p31^{comet} content in a cell, we additionally examined the effect of p31^{comet} depletion. For this purpose, three different p31^{comet} siRNAs were introduced into A549 cells (Supplementary Fig. S7A), and changes in SA-β-gal activity were monitored. On p31^{comet} depletion, there was no evidence of a phenotype displaying characteristics of senescence, such as SA-β-gal activity (Supplementary Fig. S7B) or cell growth retardation (Supplementary Fig. S7C). Finally, to confirm whether senescence by p31^{comet} results from Mad2 inhibition, we coinduced Mad2 with p31^{comet}. We found that ~2% of cells induced with Mad2 and p31^{comet} were SA-β-gal-positive, which was in contrast to 78% of control cells induced with p31^{comet} alone (Fig. 8D). These findings further indicate that Mad2 is a key mediator of p31^{comet}-induced senescence. Therefore, we suggest that p31^{comet} may induce senescence by mediating Mad2 inhibition dependent on a direct interaction of p31^{comet} and Mad2.

As shown in Fig. 5, p21$^{Waf1/Cip1}$ depletion led to cell death instead of senescence. Accordingly, we analyzed the effect of Mad2 on this phenotypic change to determine whether the observed reduction in senescent cells as shown in Fig. 8D might be due to a concomitant increase in dead cells. Unlike the marked increase in dead cell population affected by p21$^{Waf1/Cip1}$ depletion, Mad2/p31^{comet} coexpression, Mad2 depletion alone, or deletion of the Mad2 binding site in p31^{comet} did not cause significant changes in the levels of cell death (data not shown). These findings together with data on the effects of p21$^{Waf1/Cip1}$ depletion in p31^{comet}-induced senescence suggest that phenotypic conversion of p31^{comet}-induced senescence to cell death is primarily due to p21$^{Waf1/Cip1}$ and not Mad2.

Discussion

Accelerated senescence is an anticancer mechanism that inhibits unlimited cell proliferation, eventually leading to the irreversible arrest of tumor cell growth (24, 36). Senescence triggered by drugs, radiation, or oncogenes is occasionally accompanied by mitotic defects (21), but the mechanism underlying this relationship remains to be established. In this study, we show that overexpression of p31^{comet} leads to senescence-like phenotypes, such as increase in multinucleation and SA-β-gal activity (Fig. 1), permanent growth arrest (Fig. 3), and accumulation of senescence-associated marker proteins (Fig. 4) in the human cancer cell lines, A549 and Calu-1. Among the multinucleated cells (Fig. 1B; Supplementary Fig. S4B), binucleated cells were dominant, suggesting that mitotic defects leading to binucleated cells do not allow cells to divide and reenter the cycle. In addition to multinucleation, p31^{comet} generated massive chromosomal and nuclear abnormalities, including the formation of micronuclei and anaphase bridges, indicating that p31^{comet}-induced senescence was accompanied by mitotic catastrophe. In contrast to induction of senescence, p31^{comet} predominantly induced cell death, including apoptosis and necrosis, in other tumor cell lines such as HeLa and Hep3B (Fig. 2B). The cells undergoing death still exhibited mitotic catastrophe with multinucleation and micronuclei (data not shown). At present, the p31^{comet}-related mechanisms controlling cell susceptibility to senescence or apoptosis are unclear. Several DNA-damaging agents stimulate distinct responses of cancer cells depending on the dose, specifically apoptosis at high doses and senescence-like phenotype at low doses (32, 37). In view of the variations in susceptibility of specific cancer cells to drugs, low doses are sufficient to cause senescence through mitotic catastrophe but not to activate

Published OnlineFirst March 10, 2009; DOI: 10.1158/1541-7786.MCR-08-0056

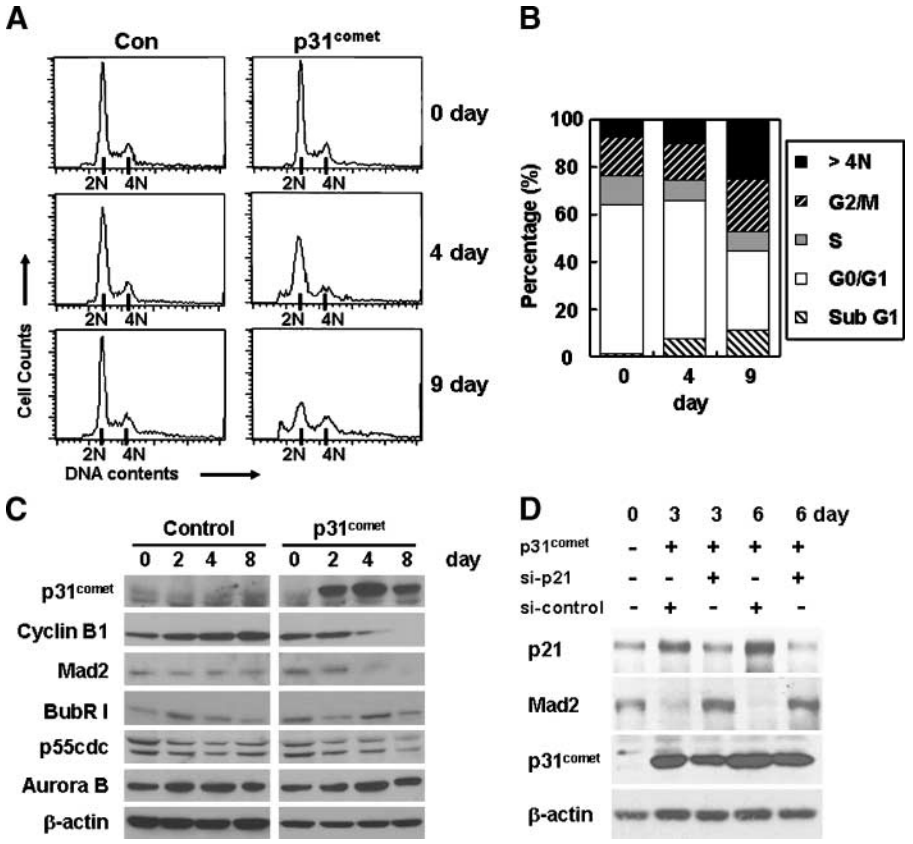

FIGURE 7. p31^{comet} transduction induces a change in distribution of the cell cycle stage. **A.** Changes in the DNA content of A549 cells infected with retroviruses containing p31^{comet} or control vector. Cells were harvested at the indicated days, and their DNA content was measured by flow cytometry. **B.** Sub-G_1 and multinuclear cells under conditions of p31^{comet} overexpression. Percentages of each cell phase were calculated by deconvolution of the DNA content histogram. **C.** Expression of spindle checkpoint regulators in cells undergoing p31^{comet}-induced senescence. A549 cells infected with retroviruses expressing p31^{comet} or control vector were harvested at the indicated times and analyzed for expression of either protein by Western blotting. **D.** Restoration of Mad2 expression by p21$^{Waf1/Cip1}$ depletion. p21$^{Waf1/Cip1}$ or p53 siRNAs were administered as described in Fig. 5, and protein levels were determined 3 and 6 d after transduction of p31^{comet}.

the apoptotic pathway. Similar to our present findings, recent studies on the molecular mechanisms of these phenotypic changes also indicate that p21$^{Waf1/Cip1}$ is a positive regulator of senescence and a negative regulator of mitotic catastrophe (38).

Prevailing evidence suggests that tumor suppressor and cell cycle inhibitor proteins are related to senescence induction and maintenance (24, 39). Overexpression of oncogenic *ras* leads to permanent cell cycle arrest in normal fibroblasts displaying distinct phenotypes from senescence (40). Our results show that permanent growth arrest by p31^{comet} differs mechanistically from that caused by oncogenic ras. Unlike oncogenic ras, p31^{comet} readily induces senescence independently of functional p53 (Figs. 4A and 5). Senescence by p31^{comet}, but not ras, is accompanied by obvious mitotic aberrations. The first direct link of abnormal mitotic checkpoints to senescence clearly defined tumor suppressors as key mediators of senescence induced by the attenuated function of mitotic checkpoint proteins. This observation rested on the surprising finding that the reduction of the BubR1 protein in natural aging is linked to senescence (15). In this context, when using mice insufficient for BubR1, p16^{Ink4a} acts as an effector and p19^{ARF} acts as an attenuator of senescence and aging (16), because the senescence- and aging-associated phenotype appears earlier through p16 depletion but later through p19 depletion. Our present study showed that, instead of accelerating or delaying senescence, p21 depletion reversed the p31^{comet}-induced phenotype from senescence to cell death without affecting mitotic catastrophe. This indicates that p21 is a major determinant of p31^{comet}-induced senescence through mitotic catastrophe. However, the elevation of p21 level is common in two other examples showing senescence through abnormal expression: BubR1 (15) and Bub3/Rae1 (17). Although these two events highlight the relatively early arrival of replicative senescence compared with that in wild-type cells, our present report emphasizes the immediate progression of senescence in tumor cells within one or two rounds of cell division after receiving p31^{comet}. In our analysis using untransformed human fibroblast cells, p31^{comet} overexpression led to immediate cell death rather than senescence.[9] These findings, together with our present results showing that p31^{comet} did not affect the level of BubR1 expression, indicate that p31^{comet} has a mechanism

[9] Unpublished data.

Published OnlineFirst March 10, 2009; DOI: 10.1158/1541-7786.MCR-08-0056

quite different from BubR1 in inducing senescence. Although the level of p53 protein was also significantly elevated together with p21, our data indicate that accumulation of p21$^{Waf1/Cip1}$, but not p53, is a prerequisite for p31^{comet}-induced senescence (Figs. 4A and 5). Although p21$^{Waf1/Cip1}$, a known target of p53, is down-regulated on p53 depletion in our experiments, p53-independent p21$^{Waf1/Cip1}$ accumulation is sufficient to induce senescence in p31^{comet}-expressing cells.

Mad2 plays a central role in regulation of the mitotic checkpoint via interactions with Cdc20, an essential accessory subunit of APC/C (4, 41-43). The importance of Mad2 in mitotic checkpoints is supported by reports that treatment with siRNA for Mad2 causes chromosome decondensation and premature sister chromatid separation, resulting in cell death (10, 44). It is plausible that p31^{comet} induces senescence through interactions with Mad2. In our present study, several lines of evidence clearly showed that p31^{comet}-induced senescence starts via Mad2 inhibition by forming complexes between them. First, the mutant lacking Mad2 binding region completely lost its ability to induce senescence. Second, both p31^{comet} overexpression and Mad2 depletion induced senescence in a similar manner. A prominent observation from the analysis of the relationship between p21$^{Waf1/Cip1}$ and Mad2 in p31^{comet}-induced senescence was that p21$^{Waf1/Cip1}$ is a key mediator of p31^{comet}-induced down-regulation of Mad2, an observation based on the fact that p21$^{Waf1/Cip1}$ depletion restored the level of Mad2 expression. This finding, together with additional result that Mad2 depletion alone also elicited

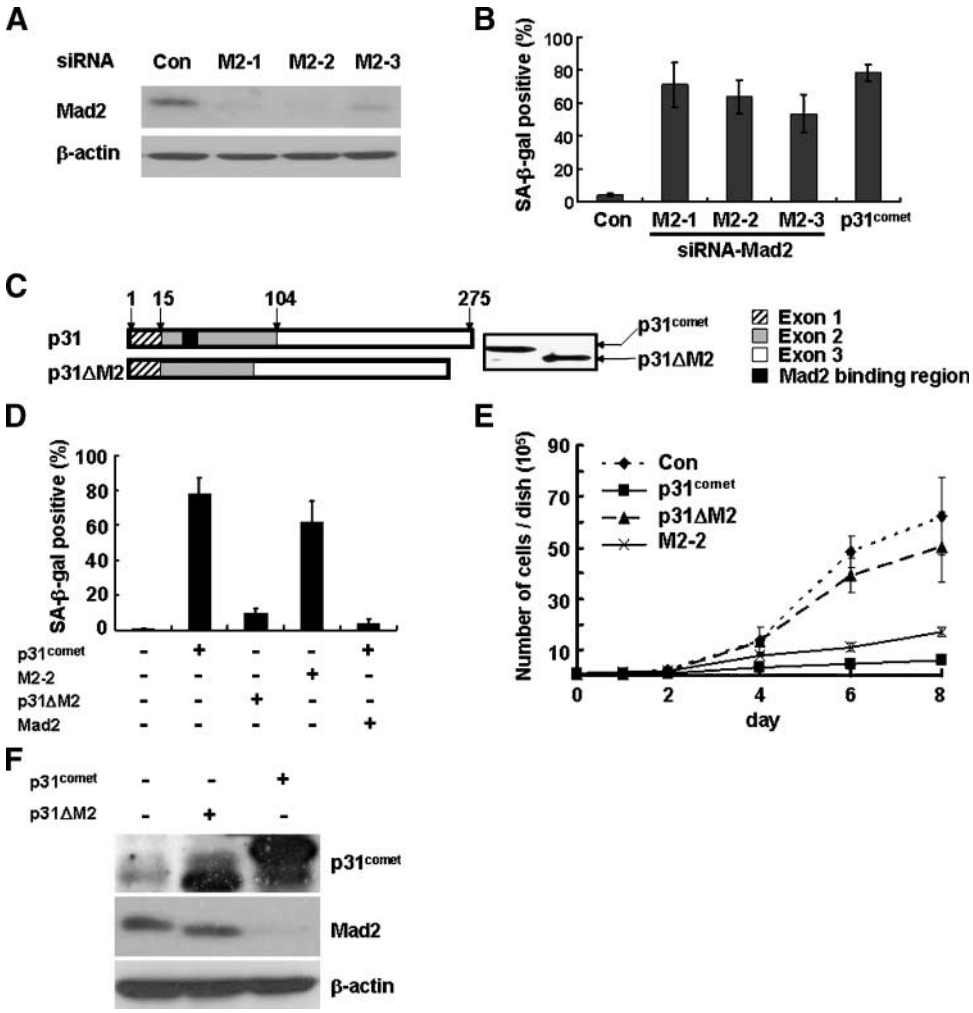

FIGURE 8. Senescence induced by p31^{comet} is dependent on Mad2 inactivation. **A.** A549 cells were transfected with Mad2 siRNA derived from three different regions of mRNA. Protein level was analyzed by Western blotting. β-Actin was used as the loading control. The numbers signify three different siRNAs. Reduced levels of Mad2 expression were calculated by scanning the band intensities. **B.** Increased SA-β-gal activity by depletion of Mad2. SA-β-gal-positive cells were scored from 400 cells per experiment 6 d after viral infection or siRNA transfection. **C.** Construction and expression of p31ΔM2 devoid of the Mad2 binding region of p31^{comet}. Levels of wild-type p31^{comet} and p31ΔM2 were compared by Western blot analysis. **D.** Induction of SA-β-gal activity by Mad2 depletion and p31^{comet} but not by p31ΔM2. A549 cells were transduced with p31^{comet}, p31ΔM2, or p31^{comet}/Mad2. For depletion of the Mad2 protein, cells were transfected with Mad2 siRNA (M2-2; present Fig. 2A). SA-β-gal-positive cells were scored as described in Fig. 2A. **E.** Growth inhibition by Mad2 depletion and overexpression of p31^{comet} but not p31ΔM2. Viable cell numbers were counted at the indicated days after virus infection or siRNA transfection. **F.** Mad2 down-regulation is not achieved by expression of p31ΔM2. Six days after the transduction of wild-type p31^{comet} or p31ΔM2, Mad2 protein levels were determined by Western blotting.

Published OnlineFirst March 10, 2009; DOI: 10.1158/1541-7786.MCR-08-0056

$p21^{Waf1/Cip1}$ up-regulation as caused by excess $p31^{comet}$ (Supplementary Fig. S6), suggests that the increased $p21^{Waf1/Cip1}$ levels via this new modulation cycle between $p31^{comet}$ and Mad2 can in turn lead to Mad2 down-regulation. Therefore, $p31^{comet}$-mediated down-regulation of Mad2 makes it possible to sustain $p21^{Waf1/Cip1}$ up-regulation.

On microtubule attachment, the $p31^{comet}$ protein specifically interacts with closed Mad2 but not open Mad2 (7, 8). Interactions between $p31^{comet}$ and the Mad2-Cdc20-APC complex lead to inhibition of Mad2 activity and subsequent activation of APC by release from the inactive state, resulting in degradation of securin and cyclin B (7, 8). Closed Mad2-$p31^{comet}$ interactions inhibit conformational changes by hindering further binding of open Mad2 to the Mad1-Mad2 core (45). Complete depletion of Mad2 results in mitotic defects by rendering the APC-Cdc20 complex free of Mad2 and dissociating Mad1 from the kinetochore followed by premature sister chromatid separation. On $p31^{comet}$ expression, most Mad1-bound Mad2 molecules interact with $p31^{comet}$ during early mitosis or G_1-G_2. This, in turn, prevents binding of Mad2 to Cdc20, a conveyable mitotic checkpoint signal, and induces continuous activation of APC/Cdc20, similar to that observed with complete Mad2 depletion. Thus, both $p31^{comet}$ expression and complete Mad2 depletion produce similar outcomes. Specifically, these include $p21^{Waf1/Cip1}$ accumulation, mitotic defects, and chromosome decondensation followed by senescence.

Based on the data presented here and in previous reports, we hypothesize that $p31^{comet}$ inhibits Mad2 function by direct interaction and accumulate $p21^{Waf1/Cip1}$. Abnormal APC activity and the resulting increased mitotic defects accumulate p53 and $p21^{Waf1/Cip1}$ proteins, and it finally resulted in senescence. Because the senescence pathway can be targeted for cancer treatment, $p31^{comet}$ serves as an effective target molecule that can be exploited to induce senescence in tumor cells. Screening the chemical library for $p31^{comet}$ up-regulation or enhanced interactions between $p31^{comet}$ and Mad2 is a feasible approach.

Materials and Methods

Cell Culture

Human cancer cell lines employed were cultured in Ham's F-12 (A549 cells), McCoy's medium (U2OS and Calu-1 cells), and MEM (Hep3B cells), respectively, supplemented with 10% fetal bovine serum and 1% penicillin-streptomycin (Life Technologies) at 37°C in a humidified 5% CO_2 incubator.

Plasmids and Antibodies

$p31^{comet}$ cDNA was amplified by PCR with sense (5′-ataaccATGGCGGCGCCGGAGGCG-3′) and antisense (5′-ccaggatccTCACTCGCGGAAGCCTTT-3′) primers using high-fidelity *Taq* polymerase (Takara). The capital letters represent nucleotides encoding $p31^{comet}$. The amplified product was digested with *Nco*I and *Bam*HI and ligated into the corresponding sites in MFG-IRES-EGFP and MFG-IRES-puro retroviral vectors. The Mad2 binding domain was deleted to generate p31ΔM2 using the QuikChange Site-Directed Mutagenesis Kit (Stratagene) using the manufacturer's protocol. The following oligonucleotides were used for site-directed mutagenesis: forward primer 5′-CAGGAAGGCTGCTGTCAGTTTACT-3′ and reverse primer 5′-TCTTGGGCAAAAGGCCTCCGAAGC-3′. p31ΔM2 was additionally subcloned into MFG-IRES-EGFP and MFG-IRES-puro retroviral vectors.

The $p31^{comet}$ antibody was generated in our laboratory by injecting purified GST-$p31^{comet}$ into rabbit. Antibodies for $p21^{Waf1/Cip1}$ (SC-397), $p27^{Kip1}$ (SC-1641), $p16^{Ink4a}$ (SC-759), p53 (SC-6243), and β-actin (SC-1616) were purchased from Santa Cruz Biotechnology, and Mad2 antibody (A300-300A) was obtained from Bethyl Laboratories.

Colony-Forming Assay

Clonogenic cell survival was evaluated with a colony-forming assay. At 1 day after virus infection, cells were plated in 100 mm dishes and incubated at 37°C. For colony formation, cells were seeded at a density of 1.5×10^3 per 10 mm dish. After 7 to 11 days of incubation, cells were fixed and stained with crystal violet. We counted total and EGFP-positive colonies containing >200 cells.

Retrovirus Production and Infection

To generate a retrovirus-producing cell line, pMFG-$p31^{comet}$ was introduced into the H29D retrovirus packaging culture by transient transfection using Lipofectamine (Invitrogen). After 72 h, supernatant fractions were harvested, and polybrene (Sigma) was added to a concentration of 6 μg/mL. Unwanted cells were removed by filtration through 0.4 μm pores. Virus titers, measured in a NIH3T3 cell line by counting EGFP-positive colony formation, were between 10^5 and 5×10^5 mL^{-1} (retrovirus-IRES-EGFP).

SA-β-gal and 4′,6-Diamidino-2-Phenylindole Double Staining

Cells were stained for β-gal activity as described earlier (22). In brief, 5×10^5 cells were seeded on a 60 mm plate 2 days after virus infection. After the indicated days, cells were washed twice with PBS, fixed in 2% formaldehyde and 0.2% glutaraldehyde for 5 min in PBS, and washed twice with PBS. This was followed by staining for 12 to 16 h in X-gal staining solution [1 mg/mL X-gal, 40 mmol/L citric acid/sodium phosphate (pH 6.0), 5 mmol/L potassium ferricyanide, 5 mmol/L potassium ferrocyanide, 150 mmol/L NaCl, 2 mmol/L $MgCl_2$]. After washing twice with PBS, cells were additionally stained with 4′,6-diamidino-2-phenylindole.

Reverse Transcription-PCR

Total RNA was extracted using the RNeasy Mini Kit (Qiagen) according to the manufacturer's protocol. RNA samples were reverse transcribed with random hexamers and the SuperScript First Strand Synthesis System (Life Technologies). cDNA was amplified using Takara *Taq* polymerase (Takara). The primer sets for osteonectin, SM22, and PAI-1 and PCR conditions are described elsewhere (32). The

Published OnlineFirst March 10, 2009; DOI: 10.1158/1541-7786.MCR-08-0056

housekeeping gene β-actin (sense 5′-atcatgtttgagaccttcaacacccc-3′ and antisense 5′-catctcttgctcgaagtccagggcga-3′; products size: 317 bp) was used as an internal control for RNA loading.

Immunoblot Analysis

Cells were washed twice with ice-cold PBS and lysed in TNN buffer [50 mmol/L Tris-HCl (pH 7.7), 150 mmol/L NaCl, 0.5% NP-40] containing protease inhibitors (10 mmol/L sodium fluoride, 2 mmol/L sodium orthovanadate, 1 mmol/L phenylmethylsulfonyl fluoride, 0.2 mmol/L EDTA, 1 mmol/L DTT, 10 μg/mL aprotinin). Lysates were cleared by centrifugation at 13,000 rpm for 10 min at 4°C. Protein concentrations were determined with the Bio-Rad protein assay kit. A 30 μg aliquot of total cell protein was subjected to 10% SDS-PAGE and transferred to Protran nitrocellulose transfer membrane (Schleicher & Schuell). After transfer, membranes were blocked in 5% milk in TBS-Tween 20 [10 mmol/L Tris-HCl (pH 8.0), 150 mmol/L NaCl, 0.05% Tween 20] for 30 min and incubated with the appropriate primary antibody in 5% milk in TBS-Tween 20 for 2 h at room temperature. Next, membranes were washed three times with TBS-Tween 20 and incubated for 1 h at room temperature in TBS-Tween 20 containing horseradish peroxidase-linked anti-immunoglobulin. After three washes in TBS-Tween 20, immunoreactive products were detected with an enhanced chemiluminescence system (Amersham).

Cell Cycle Analysis

At the indicated days after infection with retrovirus for p31^{comet} expression or control, floating and trypsinized cells were combined and then used for cell cycle analysis. The progression of cell cycle profile was analyzed by fluorescence-activated cell sorting using a Becton Dickinson FACSort flow cytometer. A cell cycle analysis program (CELLQuest; Becton Dickinson) was used to determine the percentage of cells at different stages of the cycle.

Cell Death Analysis

Cell death was determined by acridine orange-ethidium bromide double staining (46). Briefly, A549 cells transduced with p31^{comet} were costained with acridine orange and ethidium bromide and then examined under ×200 magnification using a fluorescence microscope. Counts were done by a reader blind to the experimental protocol. Cells were classified as viable, apoptotic, or necrotic population. To further investigate cell death, we used 7-amino-actinomycin D and Annexin V-PE double staining (47). A549 and HeLa cells transduced with p31^{comet} were costained with 7-amino-actinomycin D and Annexin V-PE, and dead cells were counted by flow cytometry.

siRNA Knockdown of Target Proteins and Transfection

p21$^{Waf1/Cip1}$ and p53 siRNAs were purchased from Santa Cruz Biotechnology. Two days after virus infection, 5×10^5 cells were seeded in 60 mm plates containing 2.5 mL medium. Mad2 and p31^{comet} siRNAs were generated by Invitrogen. The siRNA sequences employed were as follows: 5-AATACGGACTCACCTTGCTTG-3 (M2-1), 5-AAGTGGTGAGGTCCTGGAAAG-3 (M2-2), and 5-AAAGTGGTGAGGTCCTGGAAA-3 (M2-3) for Mad2 and 5-AAGAGACTGCATGGTACCAGT-3 (p31-1), 5-AAGCTCTACGCAGGAACCTCTCA-3 (p31-2), and 5-AAGTCGAGTTCATAGAACTC C-3 (p31-3) for p31^{comet}. Transfection was done using Lipofectamine 2000 according to the manufacturer's instructions and repeated every 72 h for a maximum of two consecutive transfections. At the indicated time points, siRNA-treated cells were collected and used for various assays.

Disclosure of Potential Conflicts of Interest

No potential conflicts of interest were disclosed.

References

1. Hoyt MA, Totis L, Roberts BT. *S. cerevisiae* genes required for cell cycle arrest in response to loss of microtubule function. Cell 1991;66:507–17.

2. Li R, Murray AW. Feedback control of mitosis in budding yeast. Cell 1991;66:519–31.

3. Amon A. The spindle checkpoint. Curr Opin Genet Dev 1999;9:69–75.

4. Fang G, Yu H, Kirschner MW. Control of mitotic transitions by the anaphase-promoting complex. Philos Trans R Soc Lond B Biol Sci 1999;354:1583–90.

5. Gorbsky GJ. Cell cycle checkpoints: arresting progress in mitosis. Bioessays 1997;19:193–7.

6. Li Y, Gorbea C, Mahaffey D, Rechsteiner M, Benezra R. MAD2 associates with the cyclosome/anaphase-promoting complex and inhibits its activity. Proc Natl Acad Sci U S A 1997;94:12431–6.

7. Habu T, Kim SH, Weinstein J, Matsumoto T. Identification of a MAD2-binding protein, CMT2, and its role in mitosis. EMBO J 2002;21:6419–28.

8. Xia G, Luo X, Habu T, Rizo J, Matsumoto T, Yu H. Conformation-specific binding of p31(comet) antagonizes the function of Mad2 in the spindle checkpoint. EMBO J 2004;23:3133–43.

9. Mapelli M, Filipp FV, Rancati G, et al. Determinants of conformational dimerization of Mad2 and its inhibition by p31^{comet}. EMBO J 2006;25:1273–84.

10. Kops GJ, Foltz DR, Cleveland DW. Lethality to human cancer cells through massive chromosome loss by inhibition of the mitotic checkpoint. Proc Natl Acad Sci U S A 2004;101:8699–704.

11. Michel L, Diaz-Rodriguez E, Narayan G, Hernando E, Murty VV, Benezra R. Complete loss of the tumor suppressor MAD2 causes premature cyclin B degradation and mitotic failure in human somatic cells. Proc Natl Acad Sci U S A 2004;101:4459–64.

12. Dobles M, Liberal V, Scott ML, Benezra R, Sorger PK. Chromosome missegregation and apoptosis in mice lacking the mitotic checkpoint protein Mad2. Cell 2000;101:635–45.

13. Wang Q, Liu T, Fang Y, et al. BUBR1 deficiency results in abnormal megakaryopoiesis. Blood 2004;103:1278–85.

14. Basu J, Bousbaa H, Logarinho E, et al. Mutations in the essential spindle checkpoint gene bub1 cause chromosome missegregation and fail to block apoptosis in drosophila. J Cell Biol 1999;146:13–28.

15. Baker DJ, Jeganathan KB, Cameron JD, et al. BubR1 insufficiency causes early onset of aging-associated phenotypes and infertility in mice. Nat Genet 2004;36:744–9.

16. Baker DJ, Perez-Terzic C, Jin F, et al. Opposing roles for p16Ink4a and p19Arf in senescence and ageing caused by BubR1 insufficiency. Nat Cell Biol 2008;10:825–36.

17. Baker DJ, Jeganathan KB, Malureanu L, Perez-Terzic C, Terzic A, van Deursen JM. Early aging-associated phenotypes in Bub3/Rae1 haploinsufficient mice. J Cell Biol 2006;172:529–40.

18. Goncalves A, Braguer D, Kamath K, et al. Resistance to Taxol in lung cancer cells associated with increased microtubule dynamics. Proc Natl Acad Sci U S A 2001;98:11737–42.

19. Jung H, Sok DE, Kim Y, Min B, Lee J, Bae K. Potentiating effect of obacunone from dictamnus dasycarpus on cytotoxicity of microtuble inhibitors, vincristine, vinblastine and Taxol. Planta Med 2000;66:74–6.

20. Manfredi JJ, Horwitz SB. Taxol: an antimitotic agent with a new mechanism of action. Pharmacol Ther 1984;25:83–125.

21. Chang BD, Broude EV, Fang J, et al. p21Waf1/Cip1/Sdi1-induced growth arrest is associated with depletion of mitosis-control proteins and leads to

Published OnlineFirst March 10, 2009; DOI: 10.1158/1541-7786.MCR-08-0056

abnormal mitosis and endoreduplication in recovering cells. Oncogene 2000;19:2165–70.

22. Dimri GP, Lee X, Basile G, et al. A biomarker that identifies senescent human cells in culture and in aging skin *in vivo*. Proc Natl Acad Sci U S A 1995;92:9363–7.

23. Taylor WR, Stark GR. Regulation of the G_2/M transition by p53. Oncogene 2001;20:1803–15.

24. Campisi J. Cellular senescence as a tumor-suppressor mechanism. Trends Cell Biol 2001;11:S27–31.

25. Alcorta DA, Xiong Y, Phelps D, Hannon G, Beach D, Barrett JC. Involvement of the cyclin-dependent kinase inhibitor p16 (INK4a) in replicative senescence of normal human fibroblasts. Proc Natl Acad Sci U S A 1996;93:13742–7.

26. Tahara H, Sato E, Noda A, Ide T. Increase in expression level of p21sdi1/cip1/waf1 with increasing division age in both normal and SV40-transformed human fibroblasts. Oncogene 1995;10:835–40.

27. Bringold F, Serrano M. Tumor suppressors and oncogenes in cellular senescence. Exp Gerontol 2000;35:317–29.

28. el-Deiry WS, Tokino T, Velculescu VE, et al. WAF1, a potential mediator of p53 tumor suppression. Cell 1993;75:817–25.

29. Li DM, Sun H. PTEN/MMAC1/TEP1 suppresses the tumorigenicity and induces G_1 cell cycle arrest in human glioblastoma cells. Proc Natl Acad Sci U S A 1998;95:15406–11.

30. Otterson GA, Kratzke RA, Coxon A, Kim YW, Kaye FJ. Absence of p16INK4 protein is restricted to the subset of lung cancer lines that retains wildtype RB. Oncogene 1994;9:3375–8.

31. Dumont P, Burton M, Chen QM, et al. Induction of replicative senescence biomarkers by sublethal oxidative stresses in normal human fibroblast. Free Radic Biol Med 2000;28:361–73.

32. Eom YW, Kim MA, Park SS, et al. Two distinct modes of cell death induced by doxorubicin: apoptosis and cell death through mitotic catastrophe accompanied by senescence-like phenotype. Oncogene 2005;24:4765–77.

33. Ruth AC, Roninson IB. Effects of the multidrug transporter P-glycoprotein on cellular responses to ionizing radiation. Cancer Res 2000;60:2576–8.

34. Roninson IB, Broude EV, Chang BD. If not apoptosis, then what? Treatment-induced senescence and mitotic catastrophe in tumor cells. Drug Resist Updat 2001;4:303–13.

35. Sledz CA, Holko M, de Veer MJ, Silverman RH, Williams BR. Activation of the interferon system by short-interfering RNAs. Nat Cell Biol 2003;5:834–9.

36. Smith JR, Pereira-Smith OM. Replicative senescence: implications for *in vivo* aging and tumor suppression. Science 1996;273:63–7.

37. Chang BD, Broude EV, Dokmanovic M, et al. A senescence-like phenotype distinguishes tumor cells that undergo terminal proliferation arrest after exposure to anticancer agents. Cancer Res 1999;59:3761–7.

38. Chan TA, Hermeking H, Lengauer C, Kinzler KW, Vogelstein B. 14-3-3σ is required to prevent mitotic catastrophe after DNA damage. Nature 1999;401:616–20.

39. Serrano M, Blasco MA. Putting the stress on senescence. Curr Opin Cell Biol 2001;13:748–53.

40. Serrano M, Lin AW, McCurrach ME, Beach D, Lowe SW. Oncogenic ras provokes premature cell senescence associated with accumulation of p53 and p16INK4a. Cell 1997;88:593–602.

41. Hwang LH, Lau LF, Smith DL, et al. Budding yeast Cdc20: a target of the spindle checkpoint. Science 1998;279:1041–4.

42. Kallio M, Weinstein J, Daum JR, Burke DJ, Gorbsky GJ. Mammalian p55CDC mediates association of the spindle checkpoint protein Mad2 with the cyclosome/anaphase-promoting complex, and is involved in regulating anaphase onset and late mitotic events. J Cell Biol 1998;141:1393–406.

43. Kim SH, Lin DP, Matsumoto S, Kitazono A, Matsumoto T. Fission yeast Slp1: an effector of the Mad2-dependent spindle checkpoint. Science 1998;279:1045–7.

44. Burds AA, Lutum AS, Sorger PK. Generating chromosome instability through the simultaneous deletion of Mad2 and p53. Proc Natl Acad Sci U S A 2005;102:11296–301.

45. Yu H. Structural activation of Mad2 in the mitotic spindle checkpoint: the two-state Mad2 model versus the Mad2 template model. J Cell Biol 2006;173:153–7.

46. Darzynkiewicz Z. Simultaneous analysis of cellular RNA and DNA content. Methods Cell Biol 1994;41:401–20.

47. van Engeland M, Nieland LJ, Ramaekers FC, Schutte B, Reutelingsperger CP. Annexin V-affinity assay: a review on an apoptosis detection system based on phosphatidylserine exposure. Cytometry 1998;31:1–9.

AACR American Association for Cancer Research

Molecular Cancer Research

p31^{comet} Induces Cellular Senescence through p21 Accumulation and Mad2 Disruption

Miyong Yun, Young-Hoon Han, Sun Hee Yoon, et al.

Mol Cancer Res 2009;7:371-382. Published OnlineFirst March 10, 2009.